Chiroclinic effect and the phase diagram of achiral polar molecules in the antiferroelectric smectic B_2 phase

Dina Jukić*
Faculty of Electrical Engineering, Computer Science and Information Technologies Osijek, J.J. Strossmayera University of Osijek, 31000 Osijek, Croatia

Mojca Čepič
Faculty of Education, University of Ljubljana, 1000 Ljubljana, Slovenia and Jožef Stefan Institute, 1000 Ljubljana, Slovenia

(Received 22 February 2019; published 26 June 2019)

The paper presents a detailed analysis of the effects of chiral doping on antiferroelectric B_2 subphases in bent core systems. The studied system exhibits the phase sequence Sm$A \leftrightarrow$ Sm$AP_A \leftrightarrow$ SmC_SP_A. The chiral dopant induces the tilt in the SmAP_A phase or the tilt modulation in the SmC_SP_A phase, which is known as the chiroclinic effect, but it also influences the stability ranges and the order of the transition between the phases. The order of the phase transition changes from a continuous for weak effects of chiral doping to discontinuous for strong effects. Competition of interactions results in changes of the phase sequences, which are resumed in the phase diagram. The method that leads to these findings, which could be used for the analysis of other similar systems, is briefly presented as well.

DOI: 10.1103/PhysRevE.99.062705

I. INTRODUCTION

Liquid crystals with polar properties are formed of molecules with very distinctive properties. Smectic layers formed of elongated chiral molecules, which are tilted away from the layer normal, are polar, as in the SmC* phase in chiral polar smectics [1]. If smectic layers are formed of molecules with a shape that hinders molecular rotation, the molecules may orient in a way that the layer becomes polar. An example is a system made of molecules with a bent core, which are not chiral, but some phases they form have polar properties [2]. First compounds with bent-shaped molecules that formed liquid crystalline phases were intentionally designed and synthesized two decades ago [3]. Several phases were found in those systems and were named B_1–B_8, where the subscript indicates the order of their identification. Experimental studies of these phases revealed that several phases actually consist of sets of subphases with different structures and macroscopic properties. Probably the most understood is the B_2 phase, in which bent core molecules are ordered in layers, and are ordered polarly in an antiferroelectric or ferroelectric way. In addition, the molecules in layers are often tilted in an anticlinic or synclinic way [4].

The B_2 phase includes six different polarly ordered subphases with different structures. Two of the phases are not tilted. Organizations of polarizations determine whether the structure is ferroelectric as in the nontilted SmAP_F phase where polarizations are parallel in adjacent layers [5], in contrast to the antiferroelectric nontilted SmAP_A phase where polarizations are antiparallel in the adjacent layers [6]. Moreover, four phases exist where molecules in the smectic layer are additionally to the polar order, also tilted. The tilts in adjacent layers in these subphases are either synclinic (SmC_SP_A, SmC_SP_F) or anticlinic (SmC_AP_A, SmC_AP_F). The combination of polar packing and molecular tilts results in the chirality of the smectic layer, although molecules are achiral. Several studies of influences of chiral dopants on these structures exist. The chiral dopant lifts the degeneracy between domains with opposite chiralities and suppresses the existence of one chirality [7]. Initially synclinic antiferroelectric structures transform to anticlinic antiferroelectric structures if chiral dopants are added. Finally, the chiroclinic effect predicts that a chiral dopant added to the nontilted polar phase induces the tilt in the nontilted SmAP_A phase [8].

In this paper we analyze how the chiral dopant added to the system influences the temperature intervals of antiferroelectric B_2 subphases' (meta)stability, their dynamics, and the order of transitions among them. The analysis is limited to the three antiferroelectric B_2 subphases, as the results can easily be adapted to the ferroelectric subphases. In addition, as long as with lowering the temperature, the first smectic phase is the nontilted polar phase, the chiral doping cannot change the polarity of the phase, but only its clinicity. Therefore, the separate analysis of the ferroelectric phases does not introduce new physics.

The most interesting system to study is the system that exhibits the phase sequence Sm$A \leftrightarrow$ Sm$AP_A \leftrightarrow$ SmC_SP_A. The chiral dopant induces the anticlinic tilt in the SmAP_A phase, but the SmC_SP_A phase that appears below is synclinic. Competition of chiral and synclinic interactions results in an interesting phase diagram, which explains observations from more

*djukic@ferit.hr

than a decade ago [7] and predicts new phenomena enabling the testing of the chiroclinic effect.

II. THE NONCHIRAL SYSTEM

The order of bent-shaped molecules is defined by two order parameters that are characteristic for the smectic layer. The first-order parameter $\vec{P}_j$ describes the ordering of the kink axes in jth layer and is always orthogonal to the layer normal (see Fig. 1). The polarization of the jth layer is proportional to the ordering of the cores' kinks; however, its direction is determined by the molecular structure and is either parallel or antiparallel to this direction. Therefore, this order parameter is called the layer polarization. The tilt order parameter $\vec{\xi}_j$ in the jth layer gives an average molecular tilt and is associated to the director in the layer (Fig. 1). The definition reflects its quadrupolar properties:

$$\vec{P}_j = \{P_{j,x}, P_{j,y}, 0\},$$
$$\vec{\xi}_j = \{n_{j,x}n_{j,z}, -n_{j,y}n_{j,z}, 0\}. \quad (1)$$

Although the two order parameters are usually considered as two dimensional, the third component is added explicitly to both for later use. Bent-shaped molecules form polarly ordered B_2 phases that are nontilted or tilted. In this study we focus on antiferroelectric structures, where the polarization order parameter has opposite directions in neighboring layers. This narrows the analysis to three possible phases: the orthogonal SmAP_A phase, the anticlinically tilted SmC_AP_A phase, and the synclinically tilted SmC_SP_A phase. The tilted

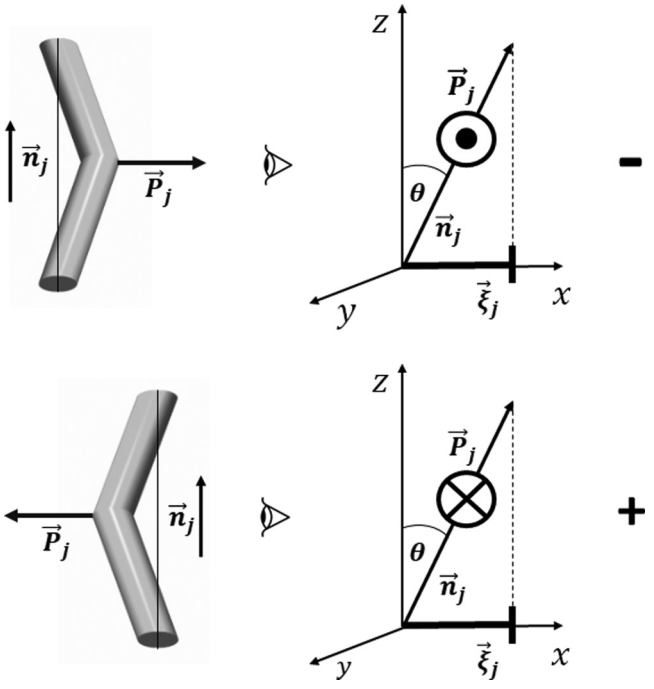

FIG. 1. Left: Schematic three-dimensional illustration of a bent-shaped molecule. Right: The symbolic presentation of the bent-shaped molecule in the coordinate system, observed from the point of view indicated by an eye, where the arrow convention is used to indicate polarization direction. The layers differ in chirality marked by ±.

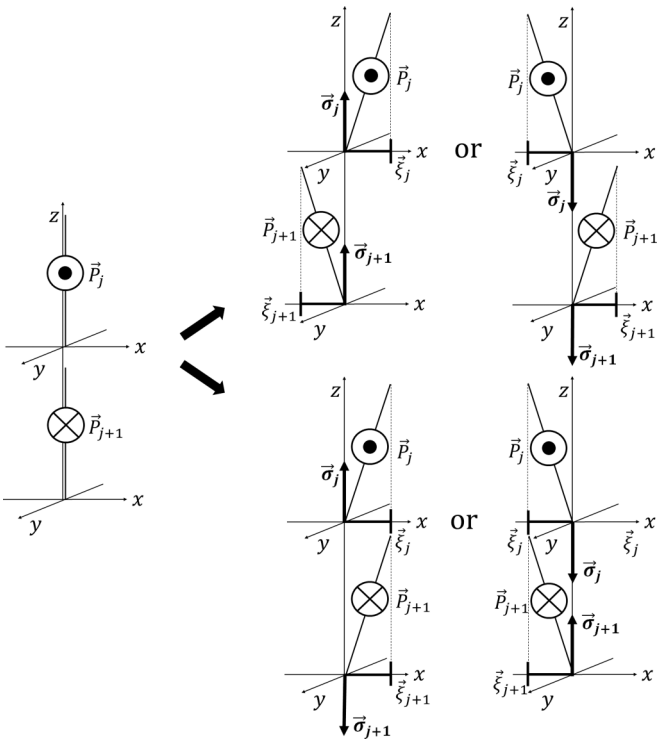

FIG. 2. Schematic illustration of possible antiferroelectric bent-shaped smectic structures. SmAP_A phase develops to one of the two energetically equivalent domains of either SmC_AP_A (top row) or SmC_SP_A phase (bottom row) upon cooling.

phases always appear below the temperature range of the nontilted phases.

Both synclinically and anticlinically tilted phases form two enantiomorphic structures. In each layer, mutual orientation of the tilt order parameter, the polarization, and the layer normal corresponds to a right-handed coordinate system, while the mirror image of these vectors corresponds to a left-handed coordinate system, indicating the chirality of the layer structure [4]. Therefore, we define a chiral order parameter of the jth layer as $\vec{\sigma}_j = \vec{P}_j \times \vec{\xi}_j$, which has the same magnitude in both cases, but the opposite signs [8,9]. The chiral order parameter is (anti)parallel to the layer normal in the local coordinate system. As only the zth component is different from zero, it has a character of the pseudoscalar, which is invariant under rotations, but changes sign under inversion, and hence disappears if the structure is achiral [10]. In the SmC_AP_A phase, which is antiferroelectric and anticlinic, all the layers have the same sign of the chiral order parameter $\vec{\sigma}_j$ and the structure is homogeneously chiral. On the contrary, in the antiferroelectric synclinic SmC_SP_A phase the signs of $\vec{\sigma}_j$ alternate from one layer to another, which indicates an antichiral structure [9]. Consequently, two homochiral domains exist in the SmC_AP_A phase and two antichiral domains in the SmC_SP_A phase with the same free energy and they occur with the same probability in samples (Fig. 2).

The free energy of a system made of achiral bent-shaped molecules expressed in the terms of order parameters, which allows for polar nontilted and polar tilted phases with chiral structures, has the following form

[11]:

$$G = \sum_j \frac{1}{2}a_{0_p}P_j^2 + \frac{1}{4}b_{0_p}P_j^4 + \frac{1}{2}a_{0_t}\xi_j^2 + \frac{1}{4}b_{0_t}\xi_j^4 + \frac{1}{2}\Omega\vec{\sigma}_{j_z}^2 + \frac{1}{2}a_{1_p}(\vec{P}_j \cdot \vec{P}_{j+1}) + \frac{1}{2}a_{1_t}(\vec{\xi}_j \cdot \vec{\xi}_{j+1}). \quad (2)$$

In Eq. (2), the subscript 0 indicates intralayer interactions, while the subscript 1 indicates interactions between neighboring layers. We do not believe that direct interactions extend to more distant layers, as the layers are well organized and strong positional correlations between molecules in next-nearest-neighboring layers are negligible [11]. The only temperature-dependent coefficient in the free energy is the first coefficient $a_{0_p} = \alpha(T - T_0)$, where T_0 is the transition temperature from the orthogonal polarly disordered to the polarly ordered phase in an isolated layer. The next three terms express van der Waals and steric interactions between molecules in the layer. The term with the negative Ω describes the coupling between the tilt and the polarization as bent-shaped molecules in the layer tilt easier in direction perpendicular to the polarization. The term with the coefficient a_{1_p} describes interactions between molecules in neighboring layers expressed in polarization. For an antiferroelectric ordering discussed in this paper, the coefficient a_{1_p} is always positive. The term with the coefficient a_{1_t} describes coupling between tilts in neighboring layers. If steric interactions, caused by partial diffusion of molecules across the layers, prevail over van der Waals attractive interactions [11], the structure favors synclinic ordering of tilts, which is described by $a_{1_t} < 0$. Otherwise, the structure is anticlinically tilted and $a_{1_t} > 0$.

To analyze the structures that minimize the free energy, we chose a domain in which the tilt order parameter has a positive direction along the x axis in the jth layer. The ansatz for the tilt and the polarization order parameters, as illustrated in Fig. 2, is

$$\begin{aligned}
&\mathrm{SmAP_A}\\
&\vec{\xi}_{0_j} = 0,\\
&\vec{P}_{0_j} = P_0\{0, 1, 0\},\\
&\vec{\xi}_{0_{j+1}} = 0,\\
&\vec{P}_{0_{j+1}} = P_0\{0, -1, 0\},\\
&\mathrm{Sm}C_SP_A\\
&\vec{\xi}_{0_j} = \theta_0\{1, 0, 0\},\\
&\vec{P}_{0_j} = P_0\{0, 1, 0\},\\
&\vec{\xi}_{0_{j+1}} = \theta_0\{1, 0, 0\},\\
&\vec{P}_{0_{j+1}} = P_0\{0, -1, 0\},\\
&\mathrm{Sm}C_AP_A\\
&\vec{\xi}_{0_j} = \theta_0\{1, 0, 0\},\\
&\vec{P}_{0_j} = P_0\{0, 1, 0\},\\
&\vec{\xi}_{0_{j+1}} = \theta_0\{-1, 0, 0\},\\
&\vec{P}_{0_{j+1}} = \theta_0\{0, -1, 0\}.
\end{aligned} \quad (3)$$

By inserting ansatz (3) in Eq. (2) a system of two linear equations for θ_0^2 and P_0^2 is obtained for the structures of the three phases

$$\begin{aligned}
&\mathrm{Sm}AP_A\\
&\theta_0 = 0,\\
&P_0^2 = -\frac{(a_{0_p} + a_{1_p})}{b_{0_p}};\\
&\mathrm{Sm}C_SP_A\\
&\theta_0^2 = -\frac{(a_{0_t} - a_{1_t})}{b_{0_t}} - \frac{\Omega}{b_{0_t}}P_0^2,\\
&P_0^2 = -\frac{(a_{0_p} + a_{1_p})}{b_{0_p}} - \frac{\Omega}{b_{0_p}}\theta_0^2;\\
&\mathrm{Sm}C_AP_A\\
&\theta_0^2 = -\frac{(a_{0_t} + a_{1_t})}{b_{0_t}} - \frac{\Omega}{b_{0_t}}P_0^2,\\
&P_0^2 = -\frac{(a_{0_p} + a_{1_p})}{b_{0_p}} - \frac{\Omega}{b_{0_p}}\theta_0^2.
\end{aligned} \quad (4)$$

III. EFFECTS OF CHIRAL DOPANTS

The temperature dependence of the tilt and polarization for an example with the sequence Sm$A \leftrightarrow$ Sm$AP_A \leftrightarrow$ SmC_SP_A is presented in Fig. 3(a). As seen in Fig. 3(a), the nontilted polar SmAP_A phase becomes stable at T_C, which is always higher than the transition temperature to a polarly ordered structure in an isolated layer. With further cooling of the sample the molecules synclinically tilt at the phase transition temperature T_S. In addition, a solution of the anticlinic SmC_AP_A phase exists below temperature T_A [Fig. 3(a)]. This additional solution stimulates a few questions. Is the SmC_AP_A phase metastable even if the system favors a synclinic ordering? Is there a mechanism that prevails over favorable synclinicity and stabilizes the anticlinic SmC_AP_A phase?

Adding a chiral dopant enhances overall chirality of the sample as interactions of bent-shaped molecules with chiral molecules favor one chiral structure and destabilize the structure with the opposite chirality [7]. Effects of chiral dopant are modeled by adding a chiral field h, which is linearly coupled with the z component of the chiral order parameter of the jth layer $h\vec{\sigma}_{j,z} = h(\vec{P}_j \times \vec{\xi}_j)_z$. The three effects of chiral dopants—a disappearance of domains with one chirality in the anticlinic SmC_AP_A phase, a modulation of amplitudes of order parameters in the SmC_SP_A phase, and an induced tilt in the nontilted SmAP_A phase, also called the chiroclinic effect—were already considered in [8]. However, for stronger chiral fields the stabilization of the anticlinic SmC_AP_A phase over the synclinic SmC_SP_A phase can be expected. Therefore, a thorough analysis of those phases under chiral doping is needed. The temperature dependence of order parameters in the chirally doped system with favorable synclinic ordering is presented in Fig. 3(b). The results were obtained numerically as the coupling with the chiral field does not allow for theoretical expressions of order parameters. Two temperature regions are clearly identified. In the temperature region

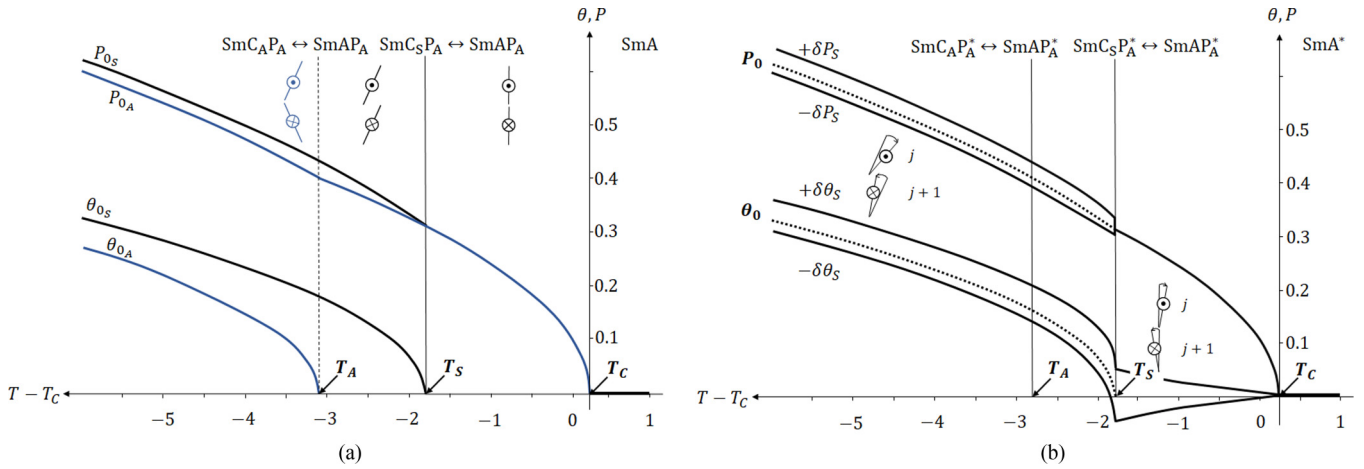

FIG. 3. Temperature dependence of order parameters in (a) pure and (b) chirally doped systems. Order parameters in the synclinic structure are marked with a subscript S, while in the anticlinic structure they are marked with an A. Vertical lines mark the phase transition temperatures. In (b) for comparison, order parameters of pure samples are presented with dotted lines. Effect of chiral dopant on tilts is symbolically illustrated with arc arrows. Structures of the phases are illustrated above the graph. Model coefficients expressed in kelvin were $b_{0_p} = 20$, $a_{0_t} = 2$, $b_{0_t} = 40$, $\Omega = -15$, $a_{1_p} = 0.2$, $a_{1_t} = -0.5$, $h = 0.15$.

between T_C and T_S, where the nontilted SmAP_A phase is stable in a system without a dopant, a chiral dopant induces tilts in opposite directions in adjacent layers. We call this phase the induced tilt SmAP_A^* phase, where the asterisk marks that the system is doped. Chiral dopant affects the synclinic SmC_SP_A phase similarly. It increases the amplitude of the tilt and the polarization in the layer with favorable chiral order parameter and decreases both order parameters in the layer with the opposite chiral order parameter. As a result, amplitudes of order parameters in odd layers differ from even ones. The modulated amplitudes of order parameters are characteristic for the chiral Sm$C_SP_A^*$ phase.

To investigate the influence of chiral dopant on stabilities of phases we analyze dynamical properties of doped structures following the procedure used in [12], as the stability limits are the most straightforwardly obtained from the fluctuation modes. The analysis is reduced to the two neighboring layers as they form a primitive cell of the structure. In the continuation, order parameters in odd layers are marked by a subscript 1 and in even layers by a subscript 2. Time-dependent order parameters in these two layers have two contributions, the stable order parameters and the thermodynamically induced fluctuations, as shown in Fig. 4:

$$\begin{aligned}
\vec{\xi}_1 &= \xi_{0_1}\,\vec{e}_{\xi_{\parallel 1}} + \delta\xi_{\parallel_1}\,\vec{e}_{\xi_{\parallel 1}} + \delta\xi_{\perp_1}\,\vec{e}_{\xi_{\perp 1}},\\
\vec{P}_1 &= P_{0_1}\,\vec{e}_{P_{\parallel 1}} + \delta P_{\parallel_1}\,\vec{e}_{P_{\parallel 1}} + \delta P_{\perp_1}\,\vec{e}_{P_{\perp 1}},\\
\vec{\xi}_2 &= \xi_{0_2}\,\vec{e}_{\xi_{\parallel 2}} + \delta\xi_{\parallel_2}\,\vec{e}_{\xi_{\parallel 2}} + \delta\xi_{\perp_2}\,\vec{e}_{\xi_{\perp 2}},\\
\vec{P}_2 &= P_{0_2}\,\vec{e}_{P_{\parallel 2}} + \delta P_{\parallel_2}\,\vec{e}_{P_{\parallel 2}} + \delta P_{\perp_2}\,\vec{e}_{P_{\perp 2}}.
\end{aligned} \tag{5}$$

The unit vectors indicate the directions of fluctuations which are parallel or perpendicular to stable order parameters in the corresponding layers $\vec{\xi}_{0_1}, \vec{P}_{0_1}$ and $\vec{\xi}_{0_2}, \vec{P}_{0_2}$, respectively (Fig. 4).

The free energy is expanded to the second order in fluctuations around the thermodynamic equilibrium. The part of the free energy due to fluctuations G_2 is shortly written as

$$G_2 = \tfrac{1}{2}\chi\,\underline{\boldsymbol{G_2}}\,\chi, \tag{6}$$

where $\chi = \{\delta\xi_{\parallel_1}, \delta\xi_{\perp_1}, \delta P_{\parallel_1}, \delta P_{\perp_1}, \delta\xi_{\parallel_2}, \delta\xi_{\perp_2}, \delta P_{\parallel_2}, \delta P_{\perp_2}\}$ is an eight-dimensional vector of fluctuation amplitudes and $\underline{\boldsymbol{G_2}}$ is an 8×8 matrix of the form

$$\underline{\boldsymbol{G_2}} = \begin{bmatrix}
A & 0 & L & 0 & I & 0 & 0 & 0\\
0 & B & 0 & K & 0 & I & 0 & 0\\
L & 0 & C & 0 & 0 & 0 & J & 0\\
0 & K & 0 & D & 0 & 0 & 0 & J\\
I & 0 & 0 & 0 & E & 0 & N & 0\\
0 & I & 0 & 0 & 0 & F & 0 & M\\
0 & 0 & J & 0 & N & 0 & G & 0\\
0 & 0 & 0 & J & 0 & M & 0 & H
\end{bmatrix}$$

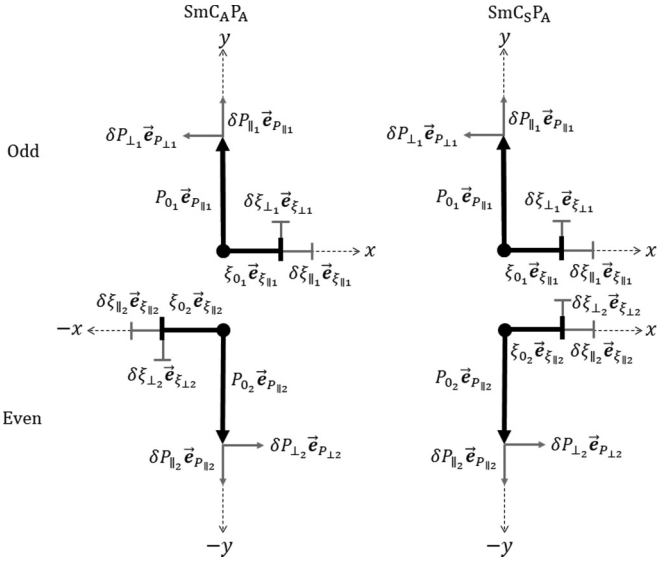

FIG. 4. Schematic presentation of fluctuations in odd and even layers of the SmC_AP_A phase and the SmC_SP_A phase.

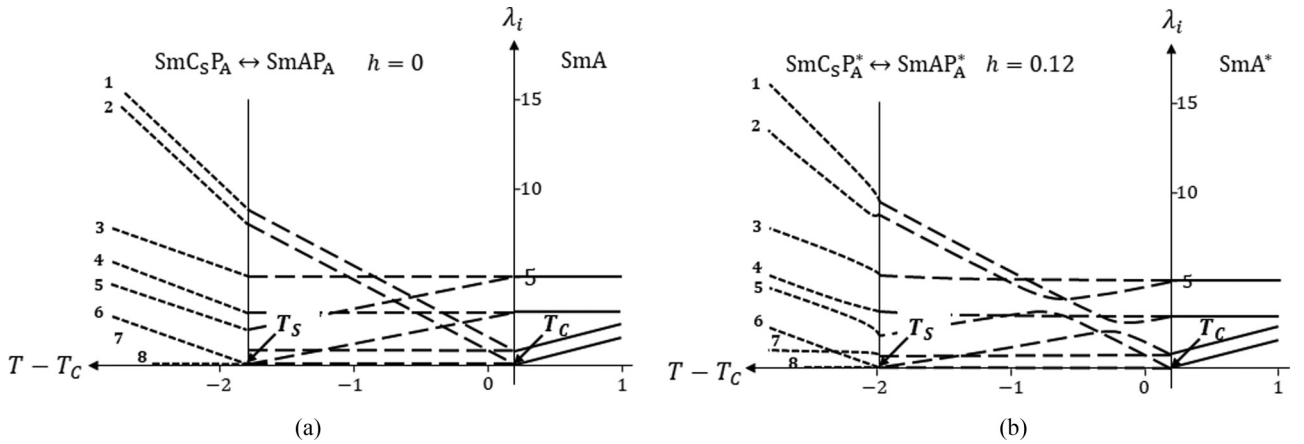

FIG. 5. Temperature dependence of the frequency of four fluctuation modes in the nontilted and eight fluctuation modes in the tilted studied phases when (a) the system is pure and (b) the system is doped with a chiral dopant. Vertical lines mark phase transitions between phases. Model coefficients are the same as in Fig. 3, while h is indicated above the graphs.

with the elements

$$A = 2a_{0_t} + 6b_{0_t}\theta_{0_1}^2 + 2\Omega P_{0_1}^2, Y$$
$$B = 2a_{0_t} + 2b_{0_t}\theta_{0_1}^2, \qquad I = \mp 2a_{1_t}$$
$$C = 2a_{0_p} + 6b_{0_p}P_{0_1}^2 + 2\Omega\theta_{0_1}^2, \qquad J = 2a_{1_p},$$
$$D = 2a_{0_p} + 2b_{0_p}P_{0_1}^2, \qquad K = 2\Omega\theta_{0_1}P_{0_1} - 2h,$$
$$E = 2a_{0_t} + 6b_{0_t}\theta_{0_2}^2 + 2\Omega P_{0_2}^2, \qquad L = 4\Omega\theta_{0_1}P_{0_1} - 2h,$$
$$F = 2a_{0_t} + 2b_{0_t}\theta_{0_2}^2, \qquad M = 2\Omega\theta_{0_2}P_{0_2}2h,$$
$$G = 2a_{0_p} + 6b_{0_p}P_{0_2}^2 + 2\Omega\theta_{0_2}^2, \qquad N = 4\Omega\,\theta_{0_2}P_{0_2} \pm 2h,$$
$$H = 2a_{0_p} + 2b_{0_p}P_{0_2}^2.$$

Stable solutions in chirally doped systems are all tilted, and they are either sinclinic ($SmC_SP_A^*$) or anticlinic ($SmAP_A^*$, $SmC_AP_A^*$). For the sinclinic structure, one uses the upper of the $\pm$ signs in matrix elements I, M, and N, while for anticlinic structures, stable tilts and polarizations are equal, and lower signs are used for I, M, and N.

In pure systems, four different fluctuation modes exist in the phases where order parameters are zero and eight fluctuation modes in the tilted phases [Fig. 5(a)]. The analysis of corresponding eigenvectors revealed that the fluctuation modes are either related to the changes of the phase or the amplitude, but never to both. In all the tilted phases, represented by dashed lines in Fig. 5, the Goldstone mode exists, reflecting the rotation symmetry of the system. Besides the Goldstone mode, three temperature-independent modes and four modes that linearly depend on temperature, exist. But, in the doped system, however, relaxation modes do not linearly depend on the temperature [Fig. 5(b)]. Furthermore, chiral dopant induces split in the amplitude modes. In addition, the analysis of the temperature dependence of the modes allows for determination of the temperature range, that is, the temperatures T_C and T_S. In this range the phases are (meta)stable, because frequencies of all modes are $\geqslant 0$.

The analysis of the model revealed that transitions $SmA \leftrightarrow SmAP_A \leftrightarrow SmC_SP_A(SmC_AP_A)$ are all continuous when the system is not doped. Adding the chiral dopant stabilizes the $SmAP_A^*$ range, the T_C increases, and the T_S decreases. Surprisingly, although the structures of $SmC_SP_A^*$ and $SmAP_A^*$ with the chiroclinically induced tilt are structurally different, the phase transition between the two phases is continuous for weak chiral fields h. However, for stronger effects of chiral dopants the phase transition becomes discontinuous.

The phase diagram for the set of coefficients given in the caption of Fig. 3, including all the subtleties, is shown in Fig. 6(a). The white region corresponds to the nontilted SmA^* phase. The light-gray region corresponds to the $SmAP_A^*$ phase with the tilt induced by the chiroclinic effect. The dark region corresponds to the $SmC_SP_A^*$ phase with slightly different tilts and polarizations in the neighboring layers, again due to the chiroclinic effect. In the semidark region, both the single chiral domain $SmC_AP_A^*$ phase and the $SmC_SP_A^*$ phase are (meta)stable. The $SmC_SP_A^*$ phase is stable below the temperatures indicated by the solid line. Along the short-dashed line the free energy of the $SmC_AP_A^*$ phase and the $SmC_SP_A^*$ phase are equal. The $SmC_AP_A^*$ phase is stable above, and the $SmC_SP_A^*$ phase is stable below this line. The metastability limit of the $SmC_AP_A^*$ phase is indicated by the long-dashed line. The dotted line indicates the limit between the spontaneously chiral anticlinic antiferroelectric phase and the dopant-induced $SmC_AP_A^*$ phase. The inset of the phase diagram in Fig. 6(a) shows the range of h where the $SmAP_A^* \leftrightarrow SmC_SP_A^*$ phase transition changes from continuous to discontinuous. A detailed analysis of temperature dependence of the lowest positive modes, marked by the long-dashed line for the $SmAP_A^*$ phase and the short-dashed line for the $SmC_SP_A^*$ phase, revealed the borders of hysteresis that exist between the h_{Low} at which transition becomes discontinuous and h_{High} for which the $SmAP_A^*$ phase remains metastable upon lowering the temperature [Fig. 6(b)]. For $h > h_{\mathrm{High}}$, the anticlinic $SmC_AP_A^*$, structurally equal to the $SmC_AP_A^*$ with high induced tilt, is (meta)stable in the whole temperature region below T_C.

How is it possible that the $SmAP_A^*$ phase with induced anticlinic tilt continuously transforms to the structurally very different sinclinically tilted $SmC_SP_A^*$ phase? Above the temperature T_S, the induced tilts in neighboring layers are opposite in direction and equal in magnitude. Directly below the phase transition at T_S, directions of tilts still remain the same, but in one layer the tilt gradually increases upon lowering the temperature and in the neighboring layer the tilt

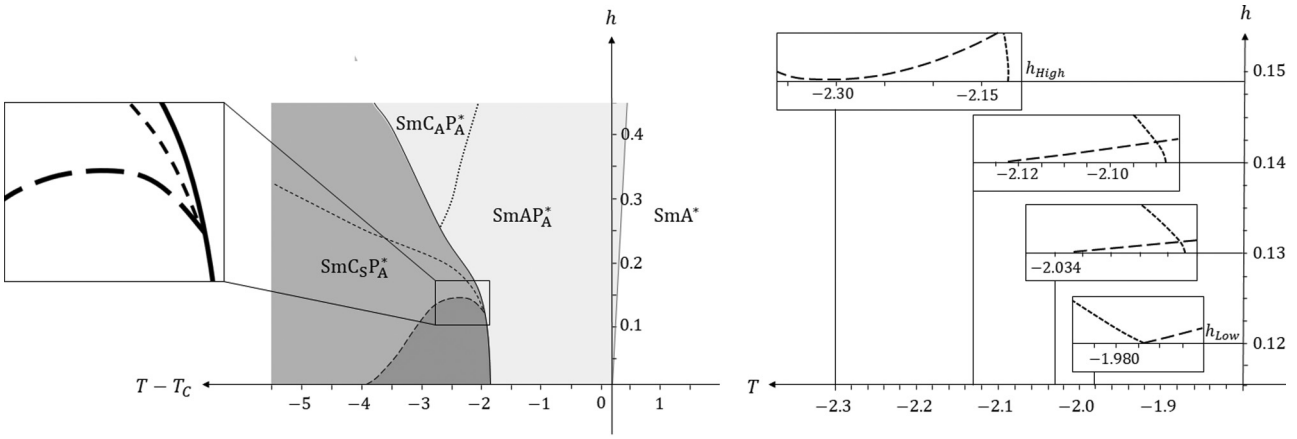

FIG. 6. Left: A phase transition temperatures and stabilities of antiferroelectric B_2 phases in dependence of the chiral field h. The inset shows a region where SmAP_A^* ↔ Sm$C_SP_A^*$ phase transition develops from continuous to discontinuous by the increase of chiral field. Right: Detailed analysis of temperature dependence of the lowest positive modes marked by a long-dashed line for the SmAP_A^* phase and a short-dashed line for the Sm$C_SP_A^*$ phase.

decreases, changes sign, and increases again, as seen in Fig. 3(b). In this way the system compensates the competition between sinclinicity favorable by diffusions through layers ($a_{1_l} < 0$) and anticlinicity favored by the chiral field h. However, if the chiral field h is too strong, the system cannot accommodate by this mechanism and the transition is discontinuous.

IV. CONCLUSIONS

In this paper we analyzed how the chiral dopant influences the temperature range of the stable phases and the order of transitions in the system that exhibits the phase sequence SmA ↔ SmAP_A ↔ SmC_SP_A. The chiral dopant induces the anticlinic tilt in the SmA_A^* phase, but the Sm$C_SP_A^*$ phase that appears below remains synclinic for weak effects of the dopant. The stability limits were deduced from the frequencies of the modes in (meta)stable structures. In the pure system, SmA ↔ SmAP_A ↔ SmC_SP_A phase transitions are continuous. In the chirally doped system, the SmA^* ↔ SmAP_A^* phase transition remains continuous. Interestingly enough, also the SmAP_A^* ↔ Sm$C_SP_A^*$ phase transition between distinctly different structures remains continuous for weak chiral fields h, but for stronger chiral field the phase transition becomes discontinuous. Inside the region where the Sm$C_SP_A^*$ phase is stable, a region exists where the Sm$C_AP_A^*$ is metastable. However, by increasing the chiral field h, the region of the stable Sm$C_AP_A^*$ phase widens, and the region of the stable Sm$C_sP_A^*$ shrinks or the phase becomes even metastable. In the region of stronger chiral fields, the electroclinically induced SmAP_A^* phase becomes indistinguishable from the spontaneously chiral anticlinically tilted Sm$C_AP_A^*$ phase.

The analysis evidently shows that adding the chiral dopant to the system stabilizes the homochiral anticlinically tilted SmC_AP_A phase in two ways. Although the sinclinicity is favored due to interlayer interactions, in the SmAP_A^* phase the anticlinic tilt is induced. Next, for strong enough chiral fields the homochiral phase becomes metastable or even stable in temperature ranges where the sinclinically tilted SmC_SP_A is stable without a dopant. As a result, the system may exhibit phase sequence SmA^* ↔ SmAP_A^* and the region with an induced tilt continuously develops to the region of a spontaneously chiral anticlinic antiferroelectric phase by tilted Sm$C_AP_A^*$ phase.

In spite of being stimulated by experiments that followed the prediction of the phenomenon [8], this study is purely theoretical. Two predictions of the model could be experimentally tested relatively easily: (a) The magnitude of the induced tilt in the SmAP_A^* phase and its temperature dependence by measuring the tilt optically, and (b) the hysteresis on heating and cooling of the doped sample using differential scanning calorimetry. The observed homochirality of domains in the Sm$C_AP_A^*$ was already discussed within this model in [8]. The effects of chiral doping, which stabilize the Sm$C_AP_A^*$ structure in the same temperature window where the Sm$C_SP_A^*$ is stable without a dopand [7] is also consistent with the part of the phase diagram, where both phases are metastable. Finally, the measurement of the tilt in dependence of the temperature in a system with the transition from SmAP_A^* to Sm$C_SP_A^*$ upon cooling, which was doped by different concentrations (up to 5%) of a chiral dopant, revealed the appearance of the tilt in the nontilted SmAP_A^* and the shift of the transition temperature to the tilted phase [13].

[1] R. Meyer, L. Liebert, L. Strzelecki, and P. Keller, J. Phys. Lett. **36**, 69 (1975).

[2] A. Jákli, O. D. Lavrentovich, and J. V. Selinger, Rev. Mod. Phys. **90**, 045004 (2018).

[3] G. Pelzl, I. Wirth, and W. Weissflog, Liq. Cryst. **28**, 969 (2001).

[4] D. R. Link, G. Natale, R. Shao, J. E. Maclennan, N. A. Clark, E. Körblova, and D. M. Walba, Science **278**, 1924 (1997).

[5] L. Guo, E. Gorecka, D. Pociecha, N. Vaupotič, M. Čepič, R. A. Reddy, K. Gornik, F. Araoka, N. A. Clark, D. M. Walba, K. Ishikawa, and H. Takezoe, Phys. Rev. E **84**, 031706 (2011).
[6] D. Pociecha, E. Gorecka, M. Čepič, N. Vaupotič, K. Gomola, and J. Mieczkowski, Phys. Rev. E **72**, 060701(R) (2005).
[7] M. Nakata, D. R. Link, F. Araoka, J. Thisayukta, Y. Takanishi, K. Ishikawa, J. Watanabe, and H. Takezoe, Liq. Cryst. **28**, 1301 (2001).
[8] M. Čepič, Europhys. Lett. **75**, 771 (2006).
[9] J. V. Selinger, Phys. Rev. Lett. **90**, 165501 (2003).
[10] A. B. Harris, R. D. Kamien, and T. C. Lubensky, Rev. Mod. Phys. **71**, 1745 (1999).
[11] M. Čepič and B. Žekš, Mol. Cryst. Liq. Cryst. Sci. Technol., Sect. A **301**, 221 (1997).
[12] D. Jukić and M. Čepič, Phase Transitions **91**, 994 (2018).
[13] M. Čepič, D. Pociecha, E. Gorecka, and W. Weissflog, in *V: Abstract Book, 11th International Conference on Ferroelectric Liquid Crystals (FLC07)* (Hokkaido University, Sapporo, Japan, 2007), p. 32.